

Fig. 1 Nomenclature for annular nozzle.

the intersection of the shroud and plug contours, respectively, with the meridional plane. The initial nozzle radii y_u and y_l , and the initial expansion contours BCC' and ADD' , are arbitrary, as are the flow properties M_i and θ_i along the noncharacteristic initial-value line AB . The stagnation temperature, pressure, and thermodynamic properties of the gas are specified. Points C and D are specified as the origin of the last right- and left-running Mach lines, respectively, of the flowfield kernel which is to be used in determining the maximum thrust contours CF and DH . The locations of points C and D are not specified in the initial problem statement, but are to be determined from the solution of the optimization problem so that the desired nozzle length is obtained. Once points C and D have been determined, the remaining initial expansion contours CC' and DD' will have no effect on the optimum nozzle contour. With this configuration, the flow net or kernel, illustrated in Fig. 1, can be generated by employing the method of characteristics for arbitrarily selected locations of points C and D .

The conditions for a maximum thrust shroud are derived first. Consider a control surface defined by the angle $\phi(y)$ in Fig. 1, which intersects the meridional plane along line EF (or $E'F'$). Point E may be chosen arbitrarily along line CK , and all the flow properties and the position coordinates of point E are known from the kernel solution. To obtain a maximum thrust shroud, the flow angle θ must be positive at point E and at every subsequent point along EF , which is the control surface for designing the shroud contour. Note that line $E'F'$ is also a possible control surface for designing the shroud contour. The only limitation is that the flow angle θ must be positive at the initial point, E or E' , chosen in the kernel.

The variational problem becomes one of maximizing the thrust F_{EF} of the shroud subject to the constraints that the mass flow rate m_{EF} be constant and that the shroud length be constant. Continuity of mass requires that the mass flow rate crossing the control surface EF be equal to the mass flow rate crossing the right-running Mach line CE .

At this point, one might question the reason for maximizing only that part of the total thrust which is generated along control surface EF , when what is really desired is the maximum total thrust for the entire nozzle. Note that the shroud contour coincides with the initial expansion contour, BC , until point C is reached. Beyond point C , the shroud contour is determined by the right-running Mach line CE and the optimizing line EF . Therefore, any changes in the flowfield due to changes in the shroud contour CF are confined to the region CEF , and do not affect the flow in the region upstream of CE . Thus, the flowfield upstream of line CE need not be considered in the variational problem.

The conditions for a maximum thrust shroud are obtained by employing the calculus of variations. The analysis is identical to that presented by Rao³ for a maximum thrust De Laval nozzle. Hence, only the results are now summarized. Along the control surface EF

$$\phi = \theta + \alpha \quad (\text{along } EF) \quad (1)$$

Equation (1) shows that the control surface EF is a left-running Mach line. On the control surface EF

$$V \cos(\theta - \alpha) / \cos \alpha = -\lambda_2 \quad (\text{along } EF) \quad (2)$$

$$y \rho V^2 \sin^2 \theta \tan \alpha = -\lambda_3 \quad (\text{along } EF) \quad (3)$$

where λ_2 and λ_3 are constant Lagrange multipliers from the variational analysis. At point F

$$\sin(2\theta) = (p - p_a) \cot \alpha / (\rho V^2 / 2) \quad (\text{at } F) \quad (4)$$

The conditions for a maximum thrust plug are identical to those derived by Rao³ for a maximum thrust spike nozzle. Consider the control surface defined by the angle $-\phi(y)$ in Fig. 1, which intersects the meridional plane along line GH (or $G'H'$). The properties and position of point G are known, and the flow angle θ is negative along GH . The mass flow rate crossing the control surface GH must be equal to the mass flow rate crossing the right-running Mach line DG . The ambient pressure thrust is a constant, and is not considered in the variational problem. The

pressure thrust on the truncated plug surface due to the base pressure p_b is included in the total plug thrust. The results obtained by Rao³ are summarized as follows. Along the control surface GH

$$\phi = \theta - \alpha \quad (\text{on } GH) \quad (5)$$

$$V \cos(-\theta - \alpha) / \cos \alpha = -\lambda_5 \quad (\text{on } GH) \quad (6)$$

$$y \rho V^2 \sin^2 \theta \tan \alpha = -\lambda_6 \quad (\text{on } GH) \quad (7)$$

$$\sin(-2\theta) = (p - p_b) \cot \alpha / (\rho V^2 / 2) \quad (\text{at } H) \quad (8)$$

where λ_5 and λ_6 are constant Lagrange multipliers from the variational analysis. Equation (5) shows that the control surface GH is a right-running Mach line.

In summary, the formulation of the maximum thrust shrouded-plug nozzle design problem is complete. For the shroud and the plug contours, the optimizing surface was found to be a left- and right-running Mach line, respectively. Two design equations were obtained on each Mach line, and a design condition was obtained at both the shroud and plug exit lip points. Those equations are sufficient to specify completely a maximum thrust shrouded-plug nozzle. In Sec. III, a numerical procedure for implementing those design equations is presented.

III. Numerical Implementation

An example is presented to illustrate the optimization procedure. The thrust maximization problem was formulated with the constraint that the length of the nozzle be a constant. Specifying the desired length thus determines a unique solution. However, the nozzle length does not enter explicitly into any of the design Eqs. (1–8). Hence, an implicit approach must be taken to solve the design equations, and the desired length is found iteratively. If either of the flow properties M or θ is specified at the nozzle exit, point F (and H), the other property can be found from the Eq. (4) [and Eq. (8)]. With these flow properties at the exit point as initial data, the design equations, together with Eq. (1) [and Eq. (5)] for the Mach line, can be solved for the location and properties along the optimizing control surface EF (and GH) in terms of the ratio y/y_F (and y/y_H). Several possible points E (and G) are generally found which match the flow properties in the kernel, and a unique point E (and G) is determined by satisfying continuity in region CEF (and DGH). Once that unique point E (and F) is determined, y_F (and y_H) can be calculated, and the nozzle length can be determined.

The preceding procedure, though straightforward, involves a large amount of computation and yields only a single optimum nozzle. That approach was followed by Rao.² A more direct approach, in which families of optimum nozzles are obtained in a single pass, is described as follows—that was followed in the present investigation. This method assumes that each point E (and G) in the kernel is the initial point on the optimizing surface for some maximum thrust nozzle. With the known properties at this point as initial data, the design equations and the Mach line equation are solved to generate the optimizing surface EF (and GH), which is terminated when continuity is satisfied. This procedure yields the flow properties (M and θ) and location (x and y) at point F (and H) directly. Equation (4) [and Eq. (8)] is then used to determine the ambient (and base) pressure for which this solution is a maximum thrust contour. A single kernel thus yields a two-dimensional array of maximum thrust nozzles with length and ambient (and base) pressure as parameters. From this array, the desired shroud contour can be chosen for any length and ambient pressure of interest. The plug contour is chosen such that the base pressure obtained from the design condition at point H matches that obtained from the actual flowfield at point H , at the desired plug length.

In the optimization of the plug contour, Eq. (8) relates the pressure at point H and the base pressure. The base pressure is an average pressure over the plug face, and it is highly dependent upon the viscous-inviscid interaction in the base region. A very simplified approach is taken wherein the base pressure is determined from an empirical model which relates the base pressure

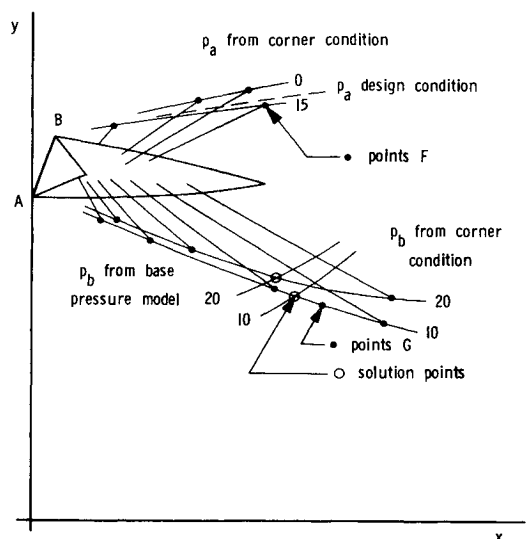


Fig. 2 Optimization map for the example case.

to the freestream properties at point H. In the present study, the following empirical model was employed:

$$p_b = p_H(C/M_H^E) \quad (9)$$

where $C = 0.846$ and $E = 1.30$. Although the base pressure was used for satisfying the corner condition, the base thrust on the truncated plug was not included in the thrust results presented in this paper, so that the results could be compared directly with those presented by Migdal.¹

For the example case, a straight, uniform, and parallel flow start line was employed with a Mach number of $M_i = 1.5$. The initial expansion contours were approximated as sharp corners by using radii of curvature of 0.01 in. The initial upper radius was $y_u = 10.0$ in., the initial lower radius was $y_l = 8.5$ in., and the initial injection angle was $\theta_i = -15^\circ$. The gas properties were $\gamma = 1.4$ and $R = 60$ (ft-lbf/lbmR). The nozzle stagnation properties were $P = 500$ psia and $T = 5000$ R. The nozzles were designed for an ambient pressure corresponding to expansion from $M_i = 1.5$ in a nozzle having an expansion ratio of 4.0, so that the results could be compared directly to the results of Migdal.¹

The solution is obtained in two steps. First, an optimization run is made as previously described to yield the array of possible shroud and plug solutions. From this array, the shroud and plug solutions to be combined into a shrouded-plug nozzle are chosen, and a second run is made to determine the properties in regions CEF and DGH for each combination, and to evaluate the shrouded-plug nozzle thrust. The number of results in the solution array depends upon the Mach line spacing in the kernel. For this example, 10 points were specified on the initial-value line, 30 points on the upper expansion surface, and 20 points on the lower expansion surface. An angular increment of 1.0° was used on both expansion surfaces to locate points from which Mach lines were initiated to generate the kernel.

The optimization map for this example case is presented in Fig. 2. Only selected right- and left-running Mach lines in the kernel are presented. Selected optimizing control surfaces are shown from the points in the kernel. Lines of constant ambient pressure as determined from the shroud design condition [Eq. (4)] are shown on the map of points F. For example, if the desired design ambient pressure is $p_a = 0.0$, then the $p_a = 0.0$ line through points F is the locus of possible shroud solutions, each having a different length. Lines of constant base pressure as determined from the plug design condition [Eq. (8)] are shown on the map of points H. Also shown are lines of constant base pressure as determined from the empirical base pressure model [Eq. (9)]. Maximum thrust plug contours are obtained where the base pressures determined by the two conditions are equal,

Table 1 Maximum thrust plug lengths

Length, in.	Length, in.
2.3724	7.0099
2.6102	7.8423
2.8679	8.8044
3.1499	9.9197
3.4608	11.2311
3.8059	12.7605
4.1911	14.5464
4.6233	16.6464
5.1107	19.0811
5.6629	20.8584
6.2912	

Table 2 Maximum thrust shroud lengths

Length, in.
2.3508
3.4131
4.9783
10.5662

denoted on the illustration as solution points. These solution points are the locus of the possible plug solutions, each having a different length. Maximum thrust shrouded-plug nozzles are then constructed by matching the desired shroud and plug solutions as selected from the optimization map. Each shroud solution can be matched with each plug solution, and vice versa, resulting in a large number of possible shrouded-plug nozzles.

From the optimization map, the optimum contours satisfying both corner conditions are identified. The results are tabulated in Tables 1 and 2. The much smaller number of shroud solutions is a result of the negative initial injection angle. As the injection angle becomes more negative, even fewer solutions exist, and eventually only plug solutions can be obtained. Shrouded-plug nozzles were obtained from the solutions presented in Tables 1 and 2 by matching each shroud solution with a plug solution of approximately the same length. For the shrouds for which no comparable length plug solution exists, a shrouded-plug combination was obtained by combining the shroud solution with two plug solutions, one longer and one shorter than the shroud, and then interpolating for the performance of the shrouded-plug combination having the length of the shroud. For the plugs which are longer than the longest shroud solution, a shrouded-

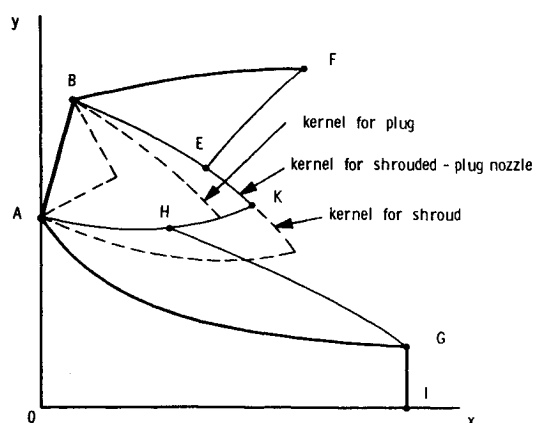


Fig. 3 Shrouded-plug nozzle performance evaluation.

Table 3 Shrouded-plug nozzle designs

Contour	Length, in.	C_F
Shroud	2.3508	1.4230
Plug	2.3724	
Shroud	3.4131	1.4727
Plug	3.4608	
Shroud	4.9783	1.5156
Plug	4.6233	
Plug	5.1107	
Shroud	10.5662	1.5737
Plug	9.9197	
Plug	11.2311	
Shroud	10.5662	1.5790
Plug	12.7605	
Shroud	10.5662	1.5829
Plug	14.5464	
Shroud	10.5662	1.5863
Plug	16.6464	
Shroud	10.5662	1.5888
Plug	19.0811	

plug combination was obtained by combining the plug solution with the longest shroud contour.

When a particular shroud and plug combination is specified, a performance run is made to determine the performance of the resulting shrouded-plug nozzle and the coordinates of the shroud and plug contours, CF and DH, respectively. This is accomplished by specifying the number of points on the upper and lower initial expansion contours so that the final kernel obtained from these points contains points E and G for the selected shroud-plug combination. Figure 3 illustrates this process. From the known solution along CE and EF, the flow properties in region CEF can be calculated and contour CF is then determined by tracing the streamline from point C to point F. Likewise, contour DH can be determined.

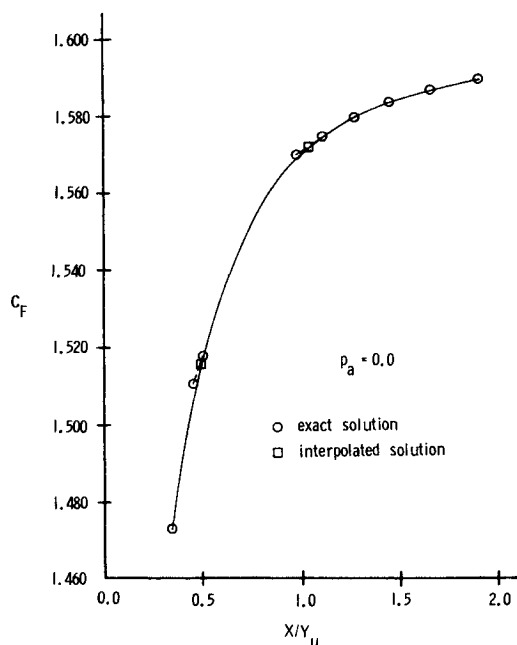


Fig. 4 Performance results for the example case.

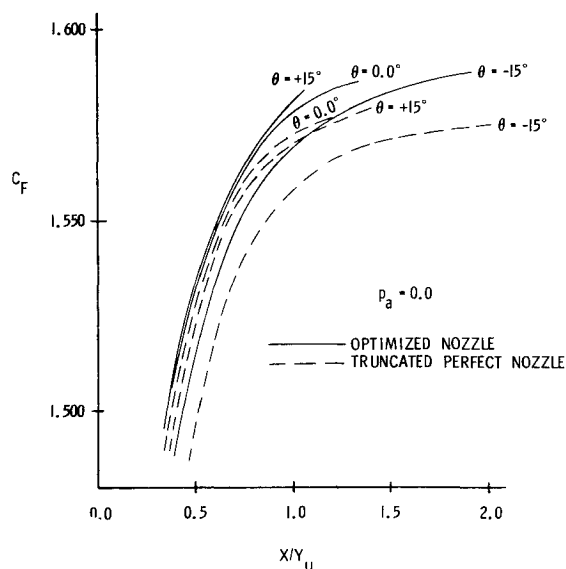


Fig. 5 Comparison of the performance of optimized and truncated perfect nozzles.

The selected shrouded-plug nozzle combinations are tabulated in Table 3, along with the resulting shrouded-plug nozzle thrust coefficients, defined as $C_F = F/P A_i$. These results are illustrated in Fig. 4. The circles represent actual solution points, while the squares represent results obtained by interpolation. The actual nozzle thrust coefficients would be somewhat larger when base thrust is included. The procedure presented here has proved very efficient for implementing the present shrouded-plug nozzle design procedure.

IV. Numerical Results

The results of a brief study of maximum thrust shrouded-plug nozzles will be presented. The nominal conditions of the study are the same as those of the example case presented in Sec. III. The sole objective of this study is to demonstrate the application of the method; no general conclusions are warranted by such a brief study.

A) Comparison with Truncated, Perfect Shrouded-Plug Nozzles

The first study compares the performance of optimized nozzles with truncated perfect shrouded-plug nozzles.¹ In both cases the design pressure ratio was that corresponding to an area ratio (exit area/inlet area) equal to 4.0. The nozzle performance was evaluated for zero ambient pressure. Figure 5 presents this comparison for injection angles of -15° , 0° , and $+15^\circ$. The -15° solution is the example presented in Sec. III. As expected, performance can be improved by optimization at all injection angles. However, as the nozzles become longer and the truncated perfect nozzle thrust coefficient approaches a maximum, the thrust coefficient curves of the two design might be expected to coincide. This is not the case, since the perfect nozzle is unduly restricted by the area ratio of 4.0. Perfect nozzles designed for larger area ratios would yield better performing truncated perfect nozzles. However, in all cases, the performance of the optimized nozzles would be superior to that of the truncated nozzles.

B. Effect of Injection Angle on Shrouded-Plug Nozzles

The injection angle at the nozzle inlet has a pronounced effect on the thrust for a given nozzle length. Results presented in Fig. 6 for shrouded-plug nozzles indicate that maximum thrust is obtained when the initial flow is axial. In this study the inner radius of the inlet was varied when the injection angle was changed to maintain a constant mass flow rate through the

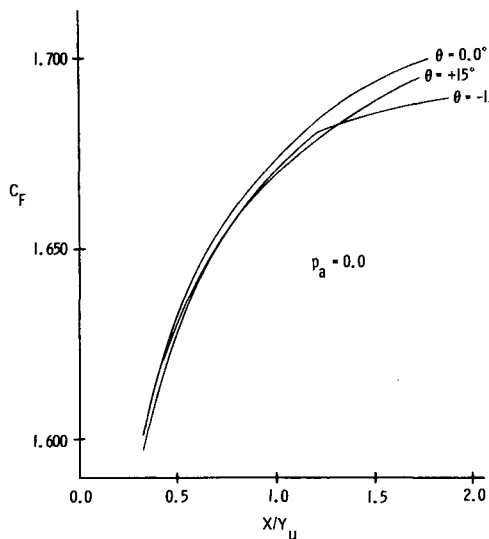


Fig. 6 Effect of injection angle on performance for a constant mass flow rate shrouded-plug nozzle.

nozzle. The nozzle is designed for a pressure ratio of 43.23, but the performance is evaluated for operation in a vacuum. For $\theta = -15.0^\circ$, the longest shroud solution available from the optimization was for $x/y_u = 1.206$. Beyond that point, only the plug is lengthened, resulting in a discontinuity in the slope of the thrust coefficient at this point and a reduced rate of thrust increase with length.

C. Effect of Injection Angle on Plug Nozzles

For large negative injection angles, few, if any, optimum shroud solutions are obtained. Figure 7 presents the performance of two families of maximum thrust plug nozzles for injection angles of -30° and -45° when no shrouds are included. As in the previous study, the inner radius of the inlet was varied when the injection angle was changed to maintain a constant mass

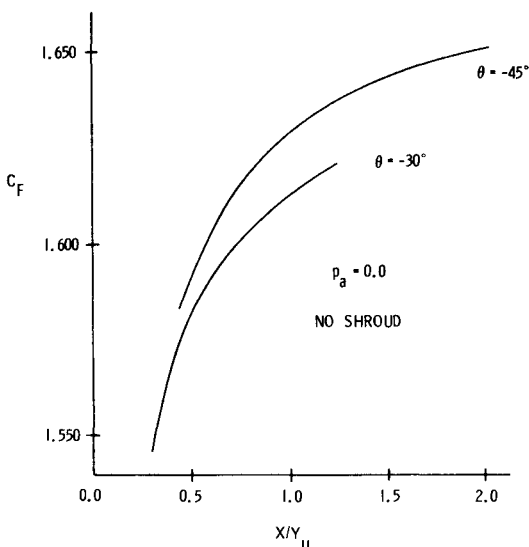


Fig. 7 Effect of injection angle on performance for a constant mass flow rate plug nozzle.

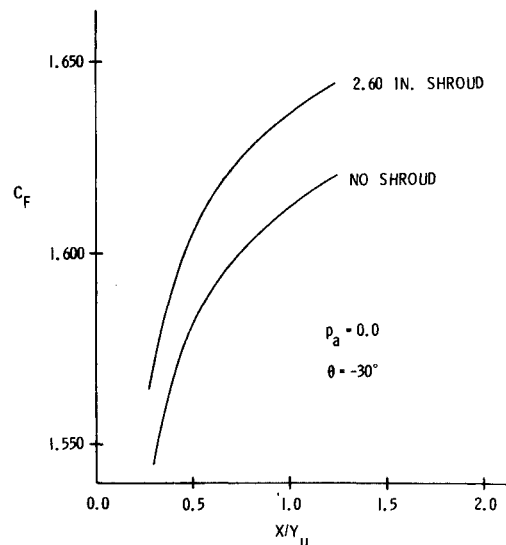


Fig. 8 Comparison of the performance of a constant mass flow rate plug and a shrouded-plug nozzle.

flow rate. The performance is greater with the larger negative injection angle, a trend opposite to that shown in Fig. 6 for shrouded-plug nozzles. This change in trend is due directly to the absence of a shroud.

D. Comparison of Plug and Shrouded-Plug Nozzles

As indicated in Sec. IV-C, the presence or absence of a shroud has a major influence on the performance trends of plug nozzles. Figure 8 presents the performance of two families of maximum thrust nozzles, one the -30° injection angle plug nozzle discussed in Fig. 7, and the other a -30° injection angle shrouded-plug nozzle. For this injection angle, the longest possible optimum shroud was 2.60 in. The upper curve in Fig. 8 presents the performance of a family of maximum thrust shrouded-plug contours all having the same 2.60 in. shroud attached. The significant performance increase over a simple plug nozzle of the same injection angle without a shroud is apparent.

V. Conclusions

A procedure has been developed for the design of shrouded-plug nozzles for maximum thrust. Such nozzles were shown to yield better performance than truncated perfect shrouded-plug nozzles. Based on a very limited study, it is clear that the injection angle and the presence of a shroud can have a significant effect on plug nozzle performance. More complete studies are needed to illustrate clearly the dependence of thrust on the various geometric parameters (that is, injection angle, upper and lower initial radii, initial expansion contours, shroud length, and plug length), and the interactions of these parameters.

References

- 1 Migdal, D., "Supersonic Annular Nozzles," *Journal of Spacecraft and Rockets*, Vol. 9, No. 1, Jan. 1972, pp. 3-6.
- 2 Rao, G. V. R., "Exhaust Nozzle Contour for Optimum Thrust," *Jet Propulsion*, Vol. 28, No. 6, June 1958, pp. 377-382.
- 3 Rao, G. V. R., "Spike Nozzle Contour for Optimum Thrust," *Ballistic Missile and Space Technology*, Vol. 2, edited by C. W. Morrow, Pergamon Press, New York, 1961, pp. 92-101.